Systems & Control Transactions

Research Article - Peer Reviewed Conference Proceeding
ESCAPE 35 - European Symposium on Computer Aided Process Engineering
Ghent, Belgium. 6-9 July 2025
Jan F.M. Van Impe, Grégoire Léonard, Satyajeet S. Bhonsale,
Monika E. Polańska, Filip Logist (Eds.)

PSE PRESS

A Physics-based, Data-driven Numerical Framework for Anomalous Diffusion of Water in Soil

Zeyuan Song[a], and Zheyu Jiang[a]*

[a] Oklahoma State University, School of Chemical Engineering, Stillwater, Oklahoma, USA
* Corresponding Author: zheyu.jiang@okstate.edu.

ABSTRACT

Precision modeling and forecasting of soil moisture are essential for implementing smart irrigation systems and mitigating agricultural drought. Most agro-hydrological models are based on the standard Richards equation, a highly nonlinear, degenerate elliptic-parabolic partial differential equation (PDE) with first order time derivative. However, research has shown that standard Richards equation is unable to model preferential flow in soil with fractal structure. In such a scenario, the soil exhibits anomalous non-Boltzmann scaling behavior. Incorporating the anomalous non-Boltzmann scaling behavior into the Richards equation leads to a generalized, time-fractional Richards equation based on fractional time derivatives. As expected, solving the time-fractional Richards equation for accurate modeling of water flow dynamics in soil faces extensive computational challenges. To target these challenges, we propose a novel numerical method that integrates finite volume method (FVM), adaptive fixed point iteration scheme, and neural network to solve the time-fractional Richards equation. Specifically, we develop an adaptive fixed point iteration scheme to solve the FVM-discretized equation iteratively, which avoids the stability issues when directly solving a stiff and sparse matrix equation. To improve the solution quality which is influenced by numerical errors and computational constraints during actual implementation, we propose to use neural networks that resemble an encoder-decoder architecture to map soil moisture profiles into a latent space and reconstruct them back. Through 1-D examples, we illustrate the accuracy and computational efficiency of our proposed physics-based, data-driven numerical method. Finally, we present a Markov chain Monte Carlo (MCMC) approach to solve the inverse problem to obtain soil-specific parameters given soil moisture solutions.

Keywords: Machine Learning, Modelling and Simulations, Numerical Methods, Water, Sustainability

INTRODUCTION

With increasing demand for food and the resulting food-energy-water nexus challenges from the growing population, there is an increasing interest among process systems engineering (PSE) researchers to design the next-generation food and agricultural systems that are sustainable, resource-efficient, and resilient. Along this line, by leveraging real-time soil monitoring technologies, sensor-based digital agriculture for sustainable and efficient use of water is essential for improving agricultural production and crop productivity and reducing agricultural droughts. To simulate the root-zone (top 1m of soil) soil moisture content, agro-hydrological models, which describe irrigation, precipitation, evapotranspiration, runoff, and drainage dynamics inside the soil, are widely used. Most existing agro-hydrological models are based on the standard Richards equation [1], which is a highly nonlinear, degenerate elliptic-parabolic partial differential equation (PDE) with first order time derivative with the form:

$$\partial_t \theta(\psi) + \nabla \cdot \boldsymbol{q} = 0, \tag{1}$$

$$\boldsymbol{q} = -(C(\theta)\nabla\theta + K(\theta)\nabla z), \tag{2}$$

where θ denotes the soil moisture content (in, e.g., $\mathrm{m}^3/\mathrm{m}^3$), $\boldsymbol{q}$ represents the water flux (in, e.g., $\mathrm{m}^3/\mathrm{m}^2 \cdot \mathrm{s}$), $K(\theta)$ is unsaturated hydraulic water conductivity (in, e.g., $\mathrm{m/s}$), $C(\theta)$ is soil moisture diffusivity (in, e.g., m^2/s), $t \in [0, t_{total}]$ denotes the time (in, e.g., s), and z corresponds to the vertical depth (in, e.g., m). For this study, without loss of generality of our proposed numerical framework, we ignore the sink term in Equation (1) associated with root water uptake. The Richards equation is a nonlinear convection-diffusion equation, where the convection term is due to gravity and the diffusion term is originated from Darcy's law. For unsaturated flow, both C and K are highly nonlinear functions of soil moisture content and soil parameters, thereby posing significant computational challenges for solving the standard Richards equation itself [2]. The integral form of the standard Richards

equation is simply given by:

$$\theta(t,\cdot) - \theta(0,\cdot) = \int_0^t \nabla \cdot (C(\theta)\nabla\theta + K(\theta)\nabla z)\mathrm{d}t, \qquad (3)$$

Besides being computationally difficult to solve, standard Richards equation is also limited when it comes to modeling realistic soil systems. For example, it has been experimentally shown that the anomalous non-Boltzmann scaling behavior is exhibited in porous media with fractal structure [3,4]. For soils exhibiting non-Boltzmann scaling behavior, the soil moisture content is a function of $\frac{\boldsymbol{x}}{t^{\frac{\alpha}{2}}}$, where $\boldsymbol{x}$ is the position vector, and α is a soil-dependent parameter indicating subdiffusion ($0 < \alpha < 1$) or superdiffusion ($1 < \alpha < 2$) [5]. Incorporating this anomalous flow behavior into the Richards equation leads to a generalized, time-fractional Richards equation:

$$\partial_t^\alpha \theta + \nabla \cdot \boldsymbol{q} = 0, \qquad (4)$$

which is even more computationally challenging due to the presence of time-fractional derivative $\partial_t^\alpha \theta$. Naïve implementations for solving Equation (4) typically involves discretizing the time-fractional Richards equation using finite difference method (FDM). However, this often causes numerical stability issues [6]. To ensure numerical stability in solving time-fractional PDEs, recent work features using a hybrid method, in which the FDM and finite element method (FEM) will be used to discretize the time and spatial domains, respectively [7]. Nevertheless, this approach was only used to solve the time-fractional fourth-order reaction-diffusion equation, where the only nonlinearity originates from the sink term. For solving the time-fractional Richards equation, a finite point method (FPM) was recently proposed to improve stability and accuracy [8]. However, this approach relies on solving the FPM scheme in matrix form, whose matrix is often stiff and sparse and hence can be difficult to solve.

To address the limitations of prevailing research, in this work, we propose a novel physics-based, data-driven numerical framework to solve time-fractional Richards equation. This framework discretizes Equation (4) using finite volume method (FVM), which inherently enforces mass conservation at the discretized level. To solve the FVM-discretized fractional Richards equation, instead of converting the discretized equations into a matrix equation, we adopt methods such as fixed point iteration scheme to convert the discretized equation system into an explicit scheme which can be solved iteratively. To enhance solution accuracy and stability, we introduce an adaptive fixed point iteration scheme that automatically selects a proper linearization constant for every iteration, time step, and discretized cell for time-fractional Richards equation based on our recent work [2]. Finally, this numerical scheme is synergistically integrated with an encoder-decoder-type architecture using simple neural networks, and the resulting data-driven, physics-embedded numerical framework achieves higher solution accuracy. This data-driven approach serves two major purposes that common numerical solvers often overlook. First, by training the neural networks using solutions obtained from solvers employing static fixed point iteration scheme under different settings (e.g., number of iterations), the encoder-decoder architecture can systematically capture and account for the numerical errors associated with realistic computational constraints (e.g., not being able to run for an infinite amount of time on a perfect computer) during actual implementation of the numerical scheme, thereby improving solution accuracy and robustness. Second, the use of data-driven approach is attractive also because it provides new opportunities for integrating physics-based modeling with online in situ soil moisture measurements for sensor-driven soil monitoring and precision agriculture applications. Commercial soil moisture sensors are not perfect and instrumental errors will always be present in their measurements. Furthermore, environmental factors (e.g., wind, temperature, evapotranspiration) and imperfect installation and maintenance will bring additional uncertainties to online soil sensing data. Thus, the data-driven approach in our numerical framework makes it amenable to leverage uncertainty-embedded dataset produced by in situ soil sensors in field environment for predictive modeling of root-zone soil moisture profiles.

Lastly, accurate estimation of soil parameters (e.g., α and C) from direct sensor measurements, also known as the inverse problem of physics-based models, is generally ill-posed due to insufficient and inaccurate measurements. Deterministic methods, which solve the inverse problem as a nonlinear optimization problem, tend to be trapped in local optima and are sensitive to data noise. Therefore, in this work, we present a probabilistic method based on Markov chain Monte Carlo (MCMC) [9] for identifying the optimal soil parameters α and C in time-fractional Richards equation given soil moisture content information as a preliminary study. Through a 1-D case study, we illustrate the effectiveness of our proposed approaches.

THE DATA-DRIVEN NUMERICAL FRAMEWORK

Approximation of time-fractional derivatives

When it comes to representing time-fractional derivatives in Equation (4), there are several options, such as Riemann-Liouville fractional integral [10,11], Caputo fractional derivative [12], fractal derivative [13], and so on. In this work, we would like to adopt the Riemann-Liouville fractional integral of the following form:

$$\mathrm{I}_{0^+}^\alpha \mathrm{f}(t) = \frac{1}{\Gamma(\alpha)} \int_0^t (t-u)^{\alpha-1} \mathrm{f}(u)\, \mathrm{d}u, \qquad (5)$$

where $\Gamma(\cdot)$ is the gamma function. With this, the integral form of time-fractional Richards equation can be expressed as:

$$\theta(t,\cdot) - \theta(0,\cdot) = \mathrm{I}_{0^+}^\alpha [\nabla \cdot (C(\theta)\nabla\theta + K(\theta)\nabla z)], \qquad (6)$$

where $\alpha > 0$. Note that the integral form of the standard Richards equation, Equation (3), is just a special case of Equation (6) by setting $\alpha = 1$.

FVM Discretization

First, we adopt an implicit Euler scheme to discretize Equation (6) in the spatial domain:

$$\theta(t_{m+1},\cdot) - \theta(t_m,\cdot) = \mathrm{I}_{0^+}^{\alpha}\left[\nabla\cdot\left(C\nabla\theta(t_{m+1},\cdot) + K\left(\theta(t_{m+1},\cdot)\right)\nabla z\right)\right] - \mathrm{I}_{0^+}^{\alpha}\left[\nabla\cdot\left(C\nabla\theta(t_m,\cdot) + K\left(\theta(t_m,\cdot)\right)\nabla z\right)\right], \quad (7)$$

where time step $m = 1,\cdots,\left\lfloor\frac{t_{total}}{\Delta t}\right\rfloor$. Next, in order to discretize Equation (6), one needs to accurately approximate Equation (5). Here, we adopt the trapezoidal quadrature formula [14] and express $\mathrm{I}_{0^+}^{\alpha}\mathrm{f}(t_{m+1})$ as:

$$\mathrm{I}_{0^+}^{\alpha}\mathrm{f}(t_{m+1}) \approx \frac{(\Delta t)^{\alpha}}{\alpha(\alpha+1)\Gamma(\alpha)}\sum_{k=0}^{m+1} a_{k,m+1}\mathrm{f}(t_{m+1}), \quad (8)$$

where the coefficient $a_{k,m+1}$ follows:

$$a_{k,m+1} = \begin{cases} m^{\alpha+1} - (m-\alpha)(m+1)^{\alpha}, & \text{if } k = 0 \\ (m-k+2)^{\alpha+1} + (m-k)^{\alpha+1} - 2(m-k+1)^{\alpha+1}, & \text{if } 1 \le k \le m \\ 1, & \text{if } k = m+1 \end{cases} \quad (9)$$

To adopt FVM, we first integrate both sides of Equation (7) over the control volume V:

$$\int_V \theta(t_{m+1},\cdot) - \theta(t_m,\cdot)\,\mathrm{d}V = \mathrm{I}_{0^+}^{\alpha}\left\{\int_V[\nabla\cdot(C(\theta)\nabla\theta(t_{m+1},\cdot) + K(\theta)\nabla z)]\,\mathrm{d}V\right\} - \mathrm{I}_{0^+}^{\alpha}\left\{\int_V[\nabla\cdot(C(\theta)\nabla\theta(t_m,\cdot) + K(\theta)\nabla z)]\,\mathrm{d}V\right\}. \quad (10)$$

Then, one can apply divergence theorem on the RHS of Equation (10), followed by discretizing the control volume V into cells V_i, where $i = 1,2,\cdots,N_i$. Each V_i is associated with surfaces $\omega_{i,j}$ for $j = 1,2,\cdots,N_{\omega_i}$, whose surface area is given by $A_{\omega_{i,j}}$. This would lead to the following FVM-discretized version of Equation (10):

$$\left(\theta_i^{m+1} - \theta_i^m\right)\mathrm{vol}(V_i) = \mathrm{I}_{0^+}^{\alpha}\left[\sum_{j=1}^{N_{\omega_i}}(C(\theta)\nabla\theta + K(\theta)\nabla z)|_{\omega_{i,j}}^{m+1}\cdot\hat{n}_{\omega_{i,j}}A_{\omega_{i,j}}\right] - \mathrm{I}_{0^+}^{\alpha}\left[\sum_{j=1}^{N_{\omega_i}}(C(\theta)\nabla\theta + K(\theta)\nabla z)|_{\omega_{i,j}}^{m}\cdot\hat{n}_{\omega_{i,j}}A_{\omega_{i,j}}\right], \quad (11)$$

where θ_i^m is a shorthand notation for the soil moisture at cell i and time step m, $|_{\omega_{i,j}}^m$ operates on surface $\omega_{i,j}$ and time step m, and $\hat{n}_{\omega_{i,j}}$denotes the outward pointing unit normal vector associated with surface $\omega_{i,j}$. Equation (8) will be used to evaluate $\mathrm{I}_{0^+}^{\alpha}[\cdot]$ in Equation (11).

Adaptive fixed point iteration scheme

In fixed point iteration scheme, for every cell i and time step $m+1$, one would multiply the fixed linearization parameter γ to Equation (11) and then add the term $\theta_i^{m+1,s+1} - \theta_i^{m+1,s}$ to either side of Equation (11), so that the Richards equation can be solved in an iterative manner to obtain the soil moisture solution upon convergence. Since γ is a static constant, a trial-and-error procedure is typically required to obtain an appropriate γ value that avoids convergence issues. Not only is this search procedure tedious to implement, the solutions obtained are also less accurate most of the time (to be shown in the case study) as the ground truth solutions are not known to us a priori. Thus, inspired by previous works [15], we introduce a novel adaptive fixed point iteration scheme that replaces the static fixed linearization parameter γ with $\gamma_i^{m+1,s}$, which adjusts itself for each specific discretized cell, time step, and iteration count s. Specifically, we introduce the term $\theta_i^{m+1,s+1} - \theta_i^{m+1,s}$ to the LHS of Equation (11). When the scheme converges for sufficiently large s, this term vanishes, which preserves the equality of Equation (11). In our previous work focusing on solving standard Richards equation [2,17], we developed a systematic procedure for choosing $\gamma_i^{m+1,s}$ that would guarantee convergence and stability of the numerical scheme. In this work, we follow the same procedure for choosing the appropriate $\gamma_i^{m+1,s}$.

Encoder-decoder-type data-driven framework

Once our adaptive linearization scheme of the FVM-discretized time-fractional Richards equation is established, we will obtain soil moisture solutions $\theta_i^{m+1,s}$ for every cell, time step, and iteration. Through the encode-decoder-type architecture, these solutions will first be mapped to their corresponding variables denoted as $\mu_i^{m+1,s}$ in a latent space via a trained neural network $\mathrm{f_{NN}}$ (i.e., $\mathrm{f_{NN}}$: $\theta_i^{m+1,s} \to \mu_i^{m+1,s}$), followed by applying inverse mapping from the latent space back to the soil moisture solutions $\hat{\theta}_i^{m+1,s}$ (which are expected to be more accurate than $\theta_i^{m+1,s}$) via another trained neural network $\mathrm{f_{NN}^{-1}}$: $\mu_i^{m+1,s} \to \hat{\theta}_i^{m+1,s}$.

The dataset used to train the two neural networks will come from two different sources/solvers. For example, during neural network training, θ solutions could be soil moisture solutions obtained from fixed point iteration scheme under different choices of linearization parameters and total iteration counts that cover their ranges expected during the actual solution process, whereas the μ solutions may come from direct sensor measurements or a simple finite difference based solver. Furthermore, we apply data augmentation to these "reference solutions" by adding zero-mean Gaussian noise with different variances [4]. After data augmentation, the resulting expanded set of reference solutions will be used for neural network training. This data augmentation step not only increases the size of the training dataset without having to actually solve the numerical schemes (thereby saving significant computational time), but also reflects the characteristics of actual soil sensing data, which are subject to various measurement uncertainties due to instrumental error, environmental uncertainties, and imperfect installation and maintenance. It turns out that introducing Gaussian noise can greatly reduce the biases of reference solutions and enhance generalization performance, thereby significantly improving the accuracy of numerical solutions.

Our data-driven adaptive fixed point iteration scheme works as follows. For a given time step m and iteration count s, $\mathrm{f_{NN}}$ first maps the $\theta_i^{m+1,s}$ to a latent space where $\mu_i^{m+1,s} = \mathrm{f_{NN}}\left(\theta_i^{m+1,s}\right)$ lies upon. The resulting adaptive linearization scheme of FVM-discretized time-fractional Richards equation in terms of $\mu_i^{m+1,s}$ is given by:

$$\mu_i^{m+1,s+1} - \mu_i^{m+1,s} = \frac{1}{\gamma_i^{m+1,s}}\left\{\mathrm{I}_{0^+}^{\alpha}\left[\sum_{j=1}^{N_{\omega_i}}(C\nabla\mu)_{\omega_{i,j}}^{m+1}\cdot\right.\right.$$

$$\hat{n}_{\omega_{i,j}} A_{\omega_{i,j}}\Big] - \mathrm{I}_{0^+}^{\alpha}\Big[\sum_{j=1}^{N_{\omega_i}} (C\nabla\mu)^m_{\omega_{i,j}} \cdot \hat{n}_{\omega_{i,j}} A_{\omega_{i,j}}\Big]\Big\} + \frac{1}{\gamma_i^{m+1,s}} \mathrm{f}_{\mathrm{NN}}(J), \quad (12)$$

where the quantity J is given by:

$$J = (\theta_i^m - \theta_i^{m+1,s})\mathrm{vol}(V_i) + \mathrm{I}_{0^+}^{\alpha}\Big[\sum_{j=1}^{N_{\omega_i}} (K(\theta)\nabla z)^{m+1}_{\omega_{i,j}} \cdot \hat{n}_{\omega_{i,j}} A_{\omega_{i,j}}\Big] - \mathrm{I}_{0^+}^{\alpha}\Big[\sum_{j=1}^{N_{\omega_i}} (K(\theta)\nabla z)^{m}_{\omega_{i,j}} \cdot \hat{n}_{\omega_{i,j}} A_{\omega_{i,j}}\Big].$$

Once $\mu_i^{m+1,s+1}$ is obtained by solving Equation (12) (which is an explicit scheme) provided $\mu_i^{m+1,s}$, we will apply the inverse mapping $\mathrm{f}_{\mathrm{NN}}^{-1}$ to transform $\mu_i^{m+1,s+1}$ from the latent space back to its original space $\hat{\theta}_i^{m+1,s+1} = \mathrm{f}_{\mathrm{NN}}^{-1}(\mu_i^{m+1,s+1})$. And the entire solution process iterates itself until a stopping criterion is reached. A commonly used stopping criterion is the relative error, which is estimated as $\varepsilon = \max_{\mathrm{i}} \frac{|\mathrm{f}_{\mathrm{NN}}^{-1}(\mu_i^{m+1,s+1}) - \mathrm{f}_{\mathrm{NN}}^{-1}(\mu_i^{m+1,s})|}{|\mathrm{f}_{\mathrm{NN}}^{-1}(\mu_i^{m+1,s+1})|}$. Or, one can specify the total number of iterations needed for each time step and cell (which is what we use for the case study).

We remark that, the two neural networks f_{NN} and $\mathrm{f}_{\mathrm{NN}}^{-1}$ can be treated as encoder and decoder, respectively, and Equation (12) essentially employs the "message passing" idea [16] via our numerical scheme.

Solving inverse problem using MCMC approach

To solve the inverse problem of identifying soil parameters, we adopt a simple MCMC approach with Metropolis-Hasting (M-H) algorithm [9]. The algorithm begins by selecting an initial set of parameters α_0. For each iteration, a candidate y is drawn from the proposal density $q(\cdot|\alpha_t)$. The acceptance probability $h(\alpha_t|y)$ is then computed. If a randomly drawn value r from the uniform distribution $\mathcal{U}([0,1])$ is less than $h(\alpha_t|y)$, the candidate y is accepted, and α_{t+1} is updated to y. Otherwise, the current parameter $\alpha_t$is retained, setting $\alpha_{t+1} = \alpha_t$. This process continues iteratively to explore the parameter space.

AN ILLUSTRATIVE EXAMPLE

In this section, we test and validate our proposed numerical framework on 1-D benchmark problem presented in [11], which features both classical and anomalous diffusion, by comparing our numerical solution with the analytical solution as well as solution obtained using fixed point iteration scheme.

1-D Classical Diffusion

For the classical diffusion problem, the parameter α is set to be 1. A constant soil moisture diffusivity $C = 24 \times 10^{-5}\ \mathrm{cm^2 min^{-1}}$ is used. The boundary condition is given by $\theta(0,t) = 0.5$ and $\theta(\infty,t) < \infty$. The initial condition is given by $\theta(z,0) = \begin{cases} 0.5, \text{if } z = 0 \\ 0.1, \text{if } z > 0 \end{cases}$. The analytical solution for this problem is $\theta(z,t) = 0.4 \cdot \mathrm{erfc}\left(\sqrt{\frac{z^2}{4Ct}}\right) + 0.1$.

Overall, we generate an augmented training dataset containing 84,480 pairs of noise-added solutions from solvers employing fixed point iteration scheme and our previously developed solver [2]. Two neural networks f_{NN} and $\mathrm{f}_{\mathrm{NN}}^{-1}$, each adopting 5 layers with 32, 64, 128, 64, 32 neurons per layer and (leaky) ReLU activation function, are trained for 10000 epochs by Adam optimizer with a learning rate of 0.001.

From the results in Figure 1 and Table 1, one can make several observations. First, solution accuracy highly depends on the choice of linearization parameters, and without the prior knowledge about where the ground truth solution lies, it will be challenging for fixed point iteration scheme to correctly identify the optimal linearization parameter to use by itself. Second, for this specific problem, since the solution quality of fixed point iteration scheme changes as $\frac{1}{\gamma}$ varies from 1 to 500, a trial-and-error process, which is both tedious and computationally expensive, will be required for identifying the optimal linearization parameter. Our proposed framework, on the other hand, does not require such trial-and-error procedure. Third, our proposed numerical framework closely matches with the analytical solution quite well, thanks to the adoption of adaptive fixed point iteration scheme and the integrated data-driven approach.

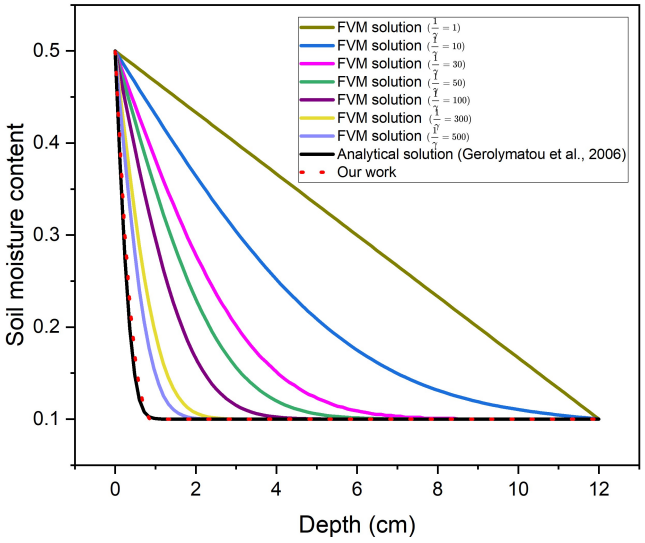

Figure 1. Numerical solutions obtained from fixed point iteration scheme and our numerical framework by setting 2,000 iterations as the stopping criterion for each time step and cell. In this example, we study the soil moisture profile across a 12-cm deep soil when $\mathrm{t_{total}} = 200$ min.

Table 1. Mean Squared Error (MSE) measuring the discrepancy between numerical solutions and the analytical solution.

Method	$\frac{1}{\gamma}$ value	MSE
FVM with a static fixed linearization parameter	1	0.0487
	10	0.0239
	30	0.0121
	50	0.0085
	100	0.0050
	300	0.0017
	500	0.0009
Our work	N/A	2.4731×10^{-5}

1-D Anomalous Diffusion

We consider the case of subdiffusion ($0 < \alpha < 1$) for anomalous diffusion problem. Again, a constant soil moisture diffusivity $C = 24 \times 10^{-5}\ \mathrm{cm^2 min^{-\alpha}}$ is used. Other the boundary and initial conditions are the same as in classical diffusion problem. The analytical solution for this problem is given by $\theta(z,t) = 0.4 \cdot \mathrm{H}_{1,1}^{1,0}\left(\sqrt{\frac{z^2}{4Ct^\alpha}}\middle|\begin{matrix}(1,\alpha/2)\\(0,1)\end{matrix}\right) + 0.1$, where $\mathrm{H}_{1,1}^{1,0}(\cdot)$ is the Fox function (see [11] for more details).

First, we solve the forward problem by considering $\alpha = 0.6$. We are mainly interested in the top 1.2 cm of soil, where the soil moisture changes significantly. From Figure 2, it is clear that, compared to the asymptote solution presented in [11], our numerical framework achieves remarkable accuracy even when simulating the region where soil moisture changes the most. Second, we investigate the performance of numerical framework in solving inverse problem when it is integrated with MCMC approach. Without informing our solver, we set the soil parameters as $\alpha = 0.13$ and $C = 24 \times 10^{-5}\ \mathrm{cm^2 min^{-\alpha}}$. We examine two scenarios, one at $t_{total} = 3$ min and the other at $t_{total} = 300$ min. Due to the ill-posedness of this inverse problem, we impose upper and lower bounds for the two parameters $0 < \alpha < 1$ and $0 < C < 30 \times 10^{-5}\ \mathrm{cm^2 min^{-\alpha}}$. The results in Figure 3 shows that the MCMC approach can estimate the soil parameters reasonably well (<20% and <1% relative discrepancy for α and C, respectively). Furthermore, it provides an error bar for the parameters being estimated, which provides basis for uncertainty quantification.

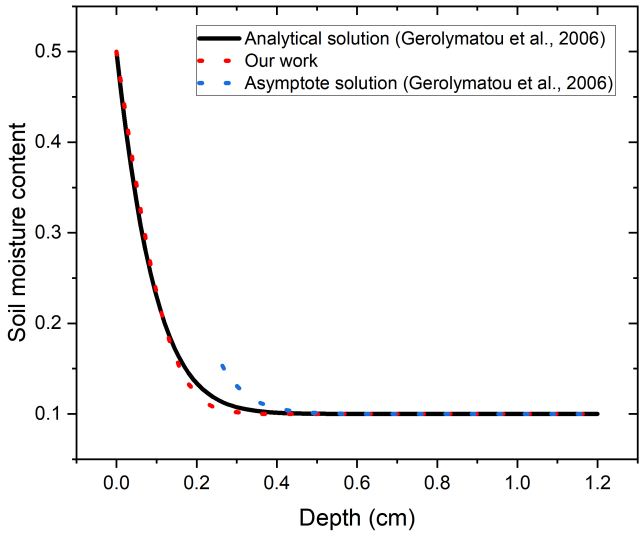

Figure 2. Solutions obtained from our numerical framework (stopping criterion: 2,000 iterations for each time step and cell) comparing to asymptote solution and analytical solution [11]. In this example, we examine the soil moisture profile across a 1.2-cm deep soil when $t_{total} = 200$ min. Here, $\alpha = 0.6$. Note that the MSE between numerical solutions from our numerical framework and analytical solution is 3.9130×10^{-6}, while that of asymptote solution is 6.7163×10^{-5}.

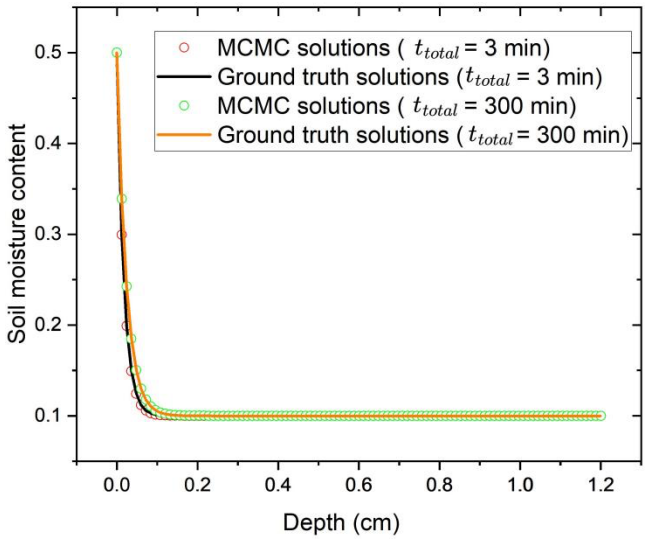

Figure 3. Numerical solutions obtained using the parameters identified by MCMC approach. Here, we conduct 1000 samplings. The resulting parameters are $\alpha = 0.13071 \pm 3.7310 \times 10^{-5}$ and $C = 23.808 \times 10^{-5} \pm 3.232 \times 10^{-12}\mathrm{cm^2 min^{-\alpha}}$. Note that the MSE between numerical solutions and desired solutions are 2.8096×10^{-8} and 7.6698×10^{-9} for $t_{total} = 3$ min and $t_{total} = 300$ min, respectively.

CONCLUSION

In this work, we develop a novel physics-based, data-driven numerical framework for simulating anomalous diffusion of water in porous media such as soil, which is characterized by the highly nonlinear time-fractional Richards equation. To address the computational challenges associated with existing solvers, we integrate neural networks and adaptive fixed point iteration scheme in a FVM discretization framework. These innovative approaches not only improves solution accuracy and robustness, but also open opportunities for integrating physics-based models with in situ soil moisture sensing technologies for precision agriculture applications. We also briefly introduce a systematic approach to solve the inverse problem using MCMC. Preliminary results obtained on a 1-D benchmark problem indicate that our proposed forward and inverse problem solvers can be highly accurate and useful. Nevertheless, we notice that one limitation of the MCMC approach for solving the inverse problem is that its accuracy highly depends on the selection of parameter bounds. In our future work, we plan to investigate other probabilistic methods that are more scalable and robust for solving inverse problems (i.e., model parameter estimation and uncertainty quantification given in situ soil moisture measurements). Overall, it is expected that this numerical framework would be integrated in an irrigation control mechanism to provide farmers with quantitative insights and recommendations regarding when to irrigate, where to irrigate, and how much to irrigate [18].

ACKNOWLEDGEMENTS

We gratefully acknowledge financial support from Oklahoma State University College of Engineering, Architecture, and Technology's Startup Fund No. 1-155160.

REFERENCES

1. Richards LA. Capillary conduction of liquids through porous mediums. Physics 1(5): 318-333 (1931) https://doi.org/10.1063/1.1745010
2. Song Z, Jiang Z. A novel numerical method for agro-hydrological modeling of water infiltration in soil. Preprint available at arXiv:2310.02806. https://doi.org/10.48550/arXiv.2310.02806
3. Ramos NM, Delgado JM, De Freitas VP. Anomalous diffusion during water absorption in porous building materials – experimental evidence. Defect and Diffusion Forum 273: 156-161 (2008) https://doi.org/10.4028/www.scientific.net/DDF.273-276.156
4. El Abd A, Abdel-Monem AM, Kansouh WA. Investigation of isothermal water infiltration into fired clay brick by scattered neutrons. J Radioanal Nucl Chem 293: 503-510 (2012) https://doi.org/10.1007/s10967-012-1788-9
5. Płociniczak Ł. Analytical studies of a time-fractional porous medium equation: Derivation, approximation, and applications. Commun Nonlinear Sci Numer Simul 24(1-3): 169-183 (2015) https://doi.org/10.1016/j.cnsns.2015.01.005
6. Meerschaert MM, Tadjeran C. Finite difference approximations for fractional advection–dispersion flow equations. J Comput Appl Math 172(1): 65-77 (2004) https://doi.org/10.1016/j.cam.2004.01.033
7. Liu Y, Du Y, Li H, He S, Gao W. Finite difference/finite element method for a nonlinear time-fractional fourth-order reaction–diffusion problem. Comput Math Appl 70(4): 573-91 (2015) https://doi.org/10.1016/j.camwa.2015.05.015
8. Qin X, Yang X. A finite point method for solving the time fractional Richards' equation, Math Probl Eng, 2019(1):8358176. https://doi.org/10.1155/2019/8358176
9. Sambridge M, Mosegaard K. Monte Carlo methods in geophysical inverse problems, Rev Geophys, 40(3):3-1 (2002) https://doi.org/10.1029/2000RG000089
10. Podlubny I. Fractional Differential Equations: An Introduction to Fractional Derivatives, Fractional Differential Equations, to Methods of Their Solution and Some of Their Applications. Elsevier (1998).
11. Gerolymatou E, Vardoulakis I, Hilfer R. Modelling infiltration by means of a nonlinear fractional diffusion model. J Phys D Appl Phys 39(18):4104 (2006) 10.1088/0022-3727/39/18/022
12. Gorenflo R., Mainardi F. Fractional Calculus: Integral and Differential Equations of Fractional Order. Springer Vienna (1997).
13. Sun H, Meerschaert MM, Zhang Y, Zhu J, Chen W. A fractal Richards' equation to capture the non-Boltzmann scaling of water transport in unsaturated media. Adv Water Resour 52:292-5 (2013) https://doi.org/10.1016/j.advwatres.2012.11.005
14. Diethelm K. Error estimates for a quadrature rule for Cauchy principal value integrals. In: Proc. Sympos. Appl. Math. Ed: Walter G. American Mathematical Society (1994)
15. Amrein M. Adaptive fixed point iterations for semilinear elliptic partial differential equations. Calcolo 56(3):30 (2019) https://doi.org/10.1007/s10092-019-0321-8
16. Brandstetter J, Worrall D, Welling M. Message passing neural PDE solvers. arXiv preprint arXiv:2202.03376 (2022)
17. Song Z, Jiang Z. A Data-driven Modeling Approach for Water Flow Dynamics in Soil, Computer Aided Chemical Engineering 52:819-824 (2023). https://doi.org/10.1016/B978-0-443-15274-0.50131-1
18. Gohar AA, Amer SA, Ward FA. Irrigation infrastructure and water appropriation rules for food security. J Hydrol 520:85-100 (2015) https://doi.org/10.1016/j.jhydrol.2014.11.036